Radio Science, Volume 25, Number 4, Pages 613–627, July–August 1990

Aspect sensitivity of stratospheric VHF radio wave scatterers, particularly above 15-km altitude

W. K. Hocking,[1] *S. Fukao, T. Tsuda, M. Yamamoto, T. Sato, and S. Kato*

Radio Atmospheric Science Center, Kyoto University, Japan

(Received May 31, 1989; revised September 27, 1989; accepted October 11, 1989.)

The aspect sensitivity of VHF radar scatter in the stratosphere is investigated with particular emphasis being placed on the region above 15-km altitude. It is found that the scatter is highly aspect sensitive below about 18 km in the stratosphere as is well known, but above this height the scatter becomes more isotropic again. The highest degree of aspect sensitivity occurs around 18-km altitude, where the backscatter polar diagram has a 1/*e* half-width θ_s of less than 1.5°, and the horizontal correlation length can exceed 30 m. At heights above 20 km, however, θ_s is in excess of 4° and increases with increasing height. At any one height there is a range of scatterer shapes, from scatterers with large length-to-depth ratios up to almost isotropic scatterers. These results are confirmed using studies of backscattered power as a function of angle, comparisons of radial velocities as a function of beam bore-tilt angle, and studies of the spectral width compared to the expected beam-broadened spectral width. The results complement and support the only other published study of scatterer anisotropy in the region of 15- to 30-km altitude (Hocking et al., 1986).

1. INTRODUCTION

Much attention has been paid to the fact that the strength of VHF radar scatter from the atmosphere is a function of beam pointing angle, with backscatter from overhead being much stronger than from the off-vertical directions. This so-called "aspect sensitivity" is very pronounced just above the tropopause. *Gage and Green* [1978] and *Roettger and Liu* [1978] were the first to report this behavior, and many studies have been made since [e.g., *Green and Gage*, 1980; *Gage et al.*, 1981; *Doviak and Zrnic*, 1984; *Tsuda et al.*, 1986; *Hocking et al.*, 1986; *Woodman and Chu*, 1989]. However, a convincing explanation of the anisotropy is still elusive. Some authors argue for the existence of steplike structures with large horizontal extent, existing either singly or in groups [e.g., *Roettger and Liu*, 1978; *Roettger*, 1980; *Gage and Green*, 1978; *Gage et al.*, 1981 (with corrections indicated by *Hocking and Roettger* [1983]), while others [e.g., *Crane*, 1980; *Doviak and Zrnic*, 1984; *Woodman and Chu*, 1989] claim that the aspect sensitivity can be explained solely by anisotropic turbulence.

It has generally been assumed that the strong aspect sensitivity exists throughout the stratosphere, but one study [*Hocking et al.*, 1986] with the sounding system (SOUSY) radar in West Germany indicated that above 20 km the aspect sensitivity begins to be less pronounced. Nevertheless, this was a single study over one 24-hour period at one particular location, and it is important to determine whether this was a unique event or whether it is a common feature at other sites, too. Only the more powerful MST radars can obtain useful echoes from above 20-km altitude, such as the SOUSY radar in West Germany and the middle and upper atmosphere (MU) radar in Japan, and so the study has been repeated with the MU radar. We have concentrated on the region above 15 km, and this therefore complements the earlier work by *Tsuda et al.* [1986], which studied aspect sensitivity with the MU radar up to a maximum of about 15-km altitude.

The purpose of this paper is to report on the results of this study. Several different methods have been used to determine the width of the polar diagram of backscatter of the scatterers, and the results of these studies and their ramifications for the small-scale dynamics of the atmosphere will be discussed in this work.

[1] On leave from University of Adelaide, Adelaide, Australia.

Paper number 89RS03282.
0048-6604/90/89RS-03282$08.00

2. EXPERIMENT

The MU radar near Kyoto in Japan is a versatile system operating at a frequency of 46.5 MHz. It has fast flexible beam steering, and it is possible to use all or subsets of the Yagi's of the main array to form a radar beam. It also features high-power and good side lobe suppression. The main beam formed when using the whole array for both transmission and reception has a half-power half-width of 1.2°. More specific details have been described by *Fukao et al.* [1985*a*, *b*].

Two separate sets of experiments were performed, the first on October 17–18, 1988 and the second on the night of December 23–24, 1988. Two distinctly different beam configurations and sampling strategies were used on these two occasions.

In the October experiment, eight beams were used with the configuration shown in Figure 1*a*. The tilt angles and azimuths were chosen so that the sampling volumes at a constant height produced a rectangular grid in the sky, as shown in Figure 1*b*. The beams were sampled on successive pulses, with the beams being sequenced in an 8-point cycle. Coherent integration over 16 points was performed giving an effective sampling time of 0.1638 s between successive points at any one height on any one beam. A 16 bit coded pulse was used to give 600-m resolution, and echoes were sampled at ranges between 7.95 and 26.55 km at 600 m intervals, giving 32 range samples in all. Data sets of 256 points were obtained between 2045 on October 17 and 0947 on October 18, each set having a duration of 42 s. A 3-s gap then followed while data transfer took place, and then the next set of 256 points was collected. Only data collected between 2045 on October 17 and 0125 on October 18 will be discussed here.

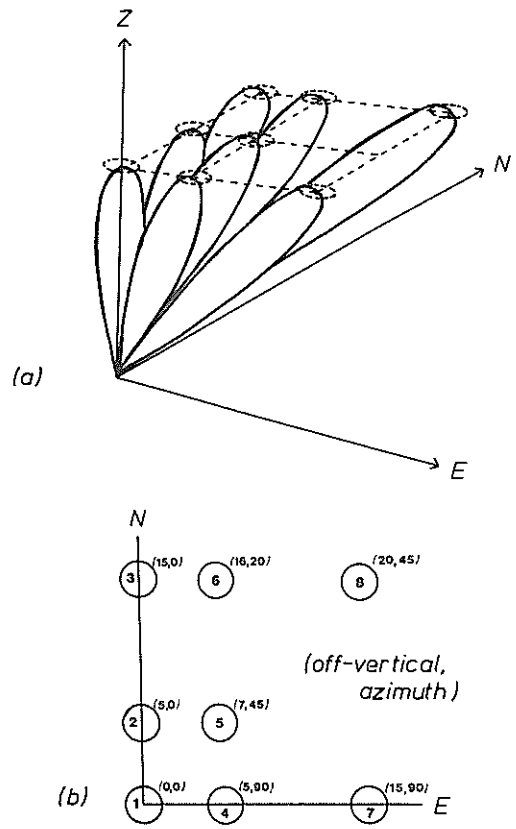

Fig. 1. (*a*) Artist's perception of the arrangement of the eight polar diagrams used in the experiment of October 17–18, 1988. The beams were chosen to form a rectangular grid at any height in the sky. The tilt angles have been exaggerated in this diagram, and as a consequence, the ranges at fixed height show greater variation as a function of beam number than was really the case. (*b*) Plan view of the regions of the sky covered by the radar at a single height. The beam configuration for the experiment of December 23–24, 1988 used one vertical beam (beam 1), one beam pointed 10° off-vertical toward the north (beam 2), and beams 3 to 8 were all pointed eastward at angles from the zenith of 4°, 8°, 12°, 16°, 20°, and 28°, respectively.

In the second experiment (December 23–24, 1988), eight beams were again used, but this time seven of the beams were in the east-west vertical plane. Again, a 600-m pulse resolution was used, but this time echoes were sampled at ranges between 13.95 and 32.55 km at 600 m intervals, again giving 32 ranges. Beam 1 was vertical, beam 2 was pointed 10° off-vertical to the north, and beams 3–8 were pointed at varying angles toward the east; namely at angles of 4°, 8°, 12°, 16°, 20°, and 28° from vertical. In this case the sampling sequence was entirely different to the October case; rather than cycle between beams on successive pulses, a complete data set of data points was collected on one beam for 42 s, and then the beam was reconfigured to the next orientation and the next data set collected. This procedure allowed more coherent integrations per sampling interval, thereby (in principle) improving the signal-to-noise ratio. In fact, 64 coherent integrations were used per point, and 512 points were collected per data set. This time the effective sampling interval was 0.082 s, or one half of that used in October. This shorter interval was used in order to help avoid the spectral aliasing anticipated on the beams which were 20° and 28°

off-vertical. Data were collected between 2200 on December 23 and 1030 on December 24, and all these data will be analyzed here.

For logistic reasons the cycling process used for the December data was relatively slow, and the total number of data sets collected was a good deal less than for the October data. The improvement in signal-to-noise was useful for determining, say, the spectra, but in fact for absolute power measurements the October data were superior because incoherent averaging of the overall means produced a marginally better signal-to-noise ratio, as will be seen later. Nevertheless, each data set served its purpose well.

3. METHOD OF ANALYSIS

3.1. *Theory*

We begin by assuming that the scatterers at any particular height have a backscatter polar diagram of the type $\exp\{-\theta^2/\theta_s^2\}$, where this represents the mean (normalized) backscattered power expected (after compensation for the differing ranges of the scatterers at different zenith angles) as a function of tilt angle for a radar beam with small half-power half-width, θ being the tilt angle of the beam. The parameter θ_s describes the degree of aspect sensitivity; it may be height dependent. A truly "specular" reflector would have θ_s approaching 0°, while isotropic scatterers would produce θ_s approaching infinity (in practice, any value in excess of about 20° can be regarded as almost isotropic). Such a polar diagram would result if the scatterers were oblate spheroids with a Gaussian increase (or decrease) in refractive index from the edge toward the center [e.g., *Briggs and Vincent*, 1973; *Hocking*, 1987]. That is, for such a model the refractive index perturbation in a single scatterer would be proportional to

$$\exp\{-x^2/L^2 - y^2/L^2 - z^2/h^2\} \tag{1}$$

where x, y, and z describe a cartesian coordinate system with z vertical. Equivalently, the autocorrelation function of the refractive index fluctuations would be equal to

$$\exp\{-\zeta_x^2/2L^2 - \zeta_y^2/2L^2 - \zeta_z^2/2h^2\} \tag{2}$$

where ζ_x, ζ_y, and ζ_z are lags in the x, y, and z directions, respectively. In fact, even if the scatterers are not ellipsoids, the autocorrelation function can still satisfy (2), and indeed at this stage, we shall make no assumption about the nature of the scattering process and regard this description merely as a parameterization. We are not necessarily rejecting "specular reflectors," for example, since these are covered by the case θ_s tending to 0°. The main advantage of this procedure is that it provides a parameterization which allows quantitative comparisons of the different degrees of "aspect sensitivity" and which can at least be related to a mathematical model of the refractive index fluctuations, something which has been lacking in some earlier more qualitative comparisons.

If one adopts this polar diagram of backscatter, then it can be shown [*Hocking et al.*, 1986; *Hocking*, 1989] that the power $P(\theta_T)$ received on an off-vertical beam relative to that on a vertical beam $P(0°)$ (where θ_T is the bore-tilt angle) is

$$\frac{P(\theta_T)}{P(0°)} = \exp\left\{-\left[\frac{(\theta_{eff}-\theta_T)^2}{\theta_0^2} + \frac{\theta_{eff}^2}{\theta_s^2}\right]\right\}\frac{h^4}{r_T^4} \tag{3}$$

Here it has been assumed that the radar polar diagram has a shape of the type $\exp\{-\theta^2/\theta_0^2\}$. The height of the scattering layer is given by h, and r_T is the range to the scattering layer on the off-vertical beam. In practice, the term h^4/r_T^4 is not too different from 1.0, at least with respect to the other terms, and will be ignored for angles less than about 10°. The parameter θ_{eff} is the effective tilt angle of the beam; it is related to θ_0 and θ_s through the relation [e.g., *Hocking*, 1989]

$$\sin\theta_{eff} = \sin\theta_T[1 + \theta_0^2/\theta_s^2]^{-1}$$

Turning (3) around, θ_s can be calculated as

$$\theta_s^2 = \frac{\theta_T^2}{R} - \theta_0^2 \tag{4}$$

where $R = \ln\{P(0)/P(\theta_T)\}$. It should also be noted that (3) corrects an error made by *Hocking et al.* [1986]. Thus measurements of power as a function of the tilt angle of the radar beam can be used to determine θ_s.

A second approach is to measure the radial velocities with off-vertical beams, and then compare them as a function of angle. For backscatter polar diagrams as described above and a tilt angle of θ_T from vertical the measured radial velocity will be R_1 times less than the radial velocity which would

have been measured if the scatter had been isotropic, where [*Hocking et al.*, 1986; *Hocking*, 1989]

$$R_1 = \left[1 + \frac{\theta_0^2}{\theta_s^2}\right]^{-1} \tag{5}$$

Measurements of R_1 therefore allow additional determinations of θ_s. If only one type of scatterer exists, R_1 will be the same at all tilt angles of the beam; but if there are several types of scatterers with different aspect-ratios, θ_s and R_1 will be functions of θ_T since different scatterer shapes will make the dominant contributions to the backscattered signal at different tilt angles. Scatterers with the largest aspect-ratios will dominate scatter from overhead, while isotropic scatterers will become more important at larger angles form the vertical.

A third analysis method which allows determination of θ_s involves examination of the spectral widths of the returned signal. If the contribution due to turbulence is negligible, as is often the case at VHF in the stratosphere [e.g., *Hocking*, 1986; *Woodman and Chu*, 1989], then the experimental spectral width will be determined by the horizontal wind speed, the polar diagram of backscatter, and the polar diagram of the radar. For a vertical pointing beam (or indeed an off-vertical beam without wind shear and for which there are no substantial variations in the horizontal velocity during the data collection period) the spectral width for isotropic scatter is

$$f_{1/2\,b} = \frac{2}{\lambda}\,\theta_{1/2(b)} V_{\text{horiz}} \tag{6}$$

where $\theta_{1/2(b)}$ is the half-power half-width of the effective radar beam (in this case the two-way beam half-width) and V_{horiz} is the horizontal wind magnitude (both horizontal components included). The half-power half-width $\theta_{(1/2)b}$ is related to the e^{-1} half-width θ_0 used previously through the relation $\theta_{(1/2)b} = \theta_0(\ln 2)^{1/2}$. If the scatterers themselves have a polar diagram of the type $\exp\{-\theta^2/\theta_s^2\}$, then the measured spectral width will be smaller than the value given by (6); in fact it will be R_2 times this where

$$R_2 = \left[1 + \frac{\theta_0^2}{\theta_s^2}\right]^{-1/2} \tag{7}$$

This formula assumes that the fluctuating motions of the scatterers do not significantly broaden the spectrum; if there is significant turbulence, the ratio may increase and even be greater than 1.0. (In that case measurements of R_2 do not allow θ_s to be determined although upper limits of θ_s are possible.) Hence by measuring the horizontal winds and the spectral widths it is possible to determine R_2 and so make a third estimate of θ_s. As will be seen, the method is not very satisfactory for off-vertical beams due to wind shears and horizontal fluctuating motions but works well with vertical beams.

All three methods are used in this paper. One further advantage of this θ_s approach is that it allows direct determinations of the length-to-depth ratio of the scatterers [e.g., *Hocking*, 1987; *Hocking et al.*, 1989]. The relevant expression is

$$[L/h]^2 = \{(\lambda^2/h)\,(8\pi^2 \sin^2\theta_s)^{-1} + 1\} \tag{8}$$

where L is the $1/e$ half-length of the scatterer and h is its $1/e$ half-depth, and we have again assumed ellipsoidal scatterers with Gaussian variations in refractive index as described in (1). The radar wavelength is denoted by λ. As shown by *Briggs and Vincent* [1973], scatterers may have a range of values of h which are capable of producing backscatter, but these h values are concentrated in a narrow range centered around about 0.2λ. Thus there is a range of (L, h) pairs which are capable of causing the same values of θ_s, but the range is not too broad. In fact, for small values of θ_s (less than about 10°), (8) can be fairly accurately written as

$$[L/h] = \{(\lambda/h)(8^{1/2}\pi \sin\theta_s)^{-1}\} \tag{9}$$

or

$$L = \lambda/(8^{1/2}\pi \sin\theta_s) \tag{10a}$$

$$L = 0.11\ \lambda/\sin\theta_s \tag{10b}$$

Thus for such small angles, θ_s gives a direct measure of the horizontal $1/e$ half-length of the scatterers. Perhaps more importantly, it gives a measure of the horizontal correlation length of the refractive index fluctuations, and this is valid even without any assumptions about the shapes of the scatterers. If L is the $1/e$ half-width, the refractive index deviation from that of the surrounding environment falls to one half its maximum at $L(\ln 2)^{1/2}$, and the autocorrelation function of the scatterer has a width $2^{1/2}$ times this. Thus the horizontal correlation length is given by

$$\zeta_{\times 0.5} = 0.13\ \lambda/\sin\ \theta_s \approx 0.13\ \lambda/\theta_s \qquad (11a)$$

if θ_s is expressed in radians, or if θ_s is expressed in degrees then

$$\zeta_{\times 0.5}/\lambda \approx 7.6/\theta_s \qquad (11b)$$

The above theory is based on the assumption of Fraunhofer (far-field) scatter. *Doviak and Zrnic* [1984] have considered the more general Fresnel case which arises for large values of L, but they concluded that this theory is only necessary for values of L in excess of 100 m for 50-MHz studies (i.e., θ_s less than about 0.5°), and we will see that this condition is rarely met in these studies. For lesser values of L the treatment above and the more exact treatment are almost identical. For example, if we use the example discussed by Doviak and Zrnic in their paper, a value for $\zeta_{\times 0.5}$ of 27 m is obtained using the above treatment, and L = 23 m. *Doviak and Zrnic* [1984, p. 331] obtained a value for their parameter "ζ_h" of 20 m. However, their parameter "ζ_h" is the same as "L" here, as can be seen by the expression used to describe the autocorrelation function in the work by *Doviak and Zrnic* [1984]. Thus their value of 20 m and the value given above of 23 m are in fairly good agreement, showing the similarity of the respective treatments. However, (11*a*) and (11*b*) are much simpler expressions than those by *Doviak and Zrnic* [1984] for determination of L, and $\zeta_{\times 0.5}$.

It should be noted at this point that the horizontal correlation lengths deduced above may not be the same values as would be determined if one were to fly a refractometer horizontally through the region because the radar measurements are only sensitive to vertical Fourier scales of one half of the radar wavelength. On the other hand, a refractometer would measure fluctuations caused by the full range of vertical Fourier scales. L is therefore a measure of the length of those scattering irregularities which backscatter the radar signals, or in other words, those scatterers with vertical extents of about one half of a radar wavelength (or more precisely, those scatterers with $h \cong 0.2\ \lambda$ if we adopt the description (1) for the shapes of the scatterers).

It is interesting to note the similarity between the autocorrelation function of the scatterers described above and the spatial correlation function of the electric field across the ground which after removal of the effects of the transmitter and receiver polar diagrams has a half-value half-width of $15.0/\theta_s$ wavelengths [e.g., *Hocking et al.*, 1989]. Apart from a numerical factor describing the width and a point-source effect which applies in the case of the diffraction pattern on the ground [e.g., *Ratcliffe*, 1956, p. 262], the two autocorrelation functions are the same, and this has in fact been shown for weak phase screens in more detail by *Booker et al.* [1950] and has been further discussed by *Briggs* [1961]. Thus measurement of the spatial autocorrelation function across the ground provides yet another way to measure L and θ_s and while not used in this paper should be borne in mind as another potentially useful technique.

3.2. *Determination of θ_s by measurements of powers*

In order to satisfactorily measure θ_s using (4) it is of course necessary to first remove the noise. In order to do this it is important to know just how well behaved the noise is. Figure 2*a* shows the time variation of the mean power (using 42-s means) as a function of time at a range of 24.2 km for the October data. At this range, most of the power is due to noise, but there is some signal at 0000–0030 hour on the vertical beam. There are, however, some large spikes in the data, and these were due to the occurrence of aircraft. This particular height was the one most affected by these. Clearly, such spikes must be removed if the analysis is to be properly performed, and Figure 2*b* shows the variation in power at a range of 26.5 km, the highest range recorded, after the removal of such spikes. The received power is all due to noise at this range, and furthermore, the mean noise fluctuations are very well behaved. The noise levels on all beams are very similar and show similar levels of fluctuation.

Figure 3 shows a typical histogram of the frequency of occurrence of particular noise levels as a function of the noise level. Noise-level histograms for the other beams showed similar distributions, with the mean power level varying generally by less than about 30% from the value shown in Figure 3. The standard deviations σ of the noise distributions were typically 0.15×10^{-9}, and the distributions were close to Gaussian in shape. This shape is important, because it allows us to apply standard statistical theory. It means, for example, that we can be confident that any measured mean power

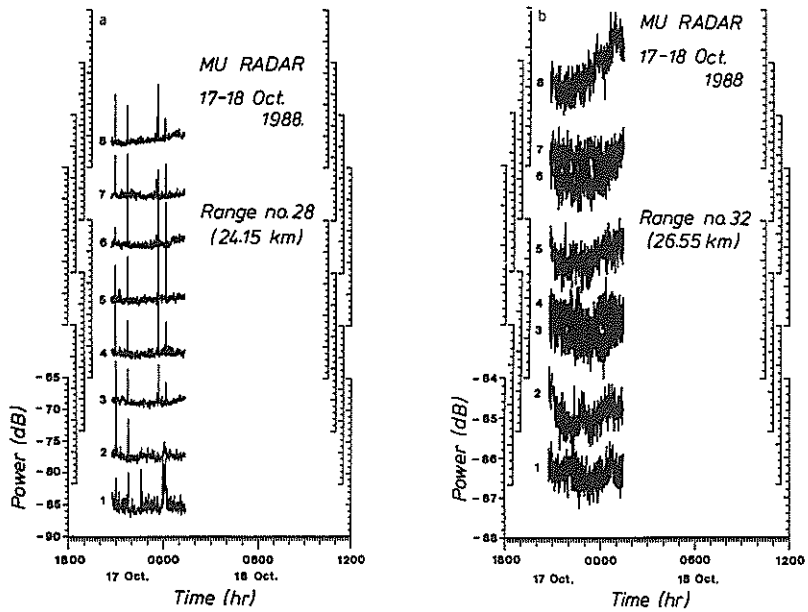

Fig. 2. (*a*) Mean power as a function of time on the 8 beams at range 28 (24.15 km) for the October 17–18 data. The effect of aircraft can clearly be seen as the large spikes. (*b*) After removal of data contaminated by aircraft the signal shows no such dramatic variations, and the mean values are much more predictable. This figure shows the power (42 s means as a function of time at range 32 (26.55 km)). In this case, all the observed power is due to noise.

produced by averaging N such 42 s means will have a 95% probability of being within $1.96\sigma/\sqrt{N}$ of the true mean. It is this well-behaved nature of the noise which makes the following analysis possible, and it is because of this that we have spent a little time studying the noise characteristics.

In subsequent analyses the noise was always subtracted from the received power, to give an estimate of the true signal. The standard error in any such measurement can be taken as $\sigma/\sqrt{N}$, N being the number of points used to form the mean power in the first place. If the signal was less than about 7 times this standard error, the data were rejected. This represents a high level of confidence, even though the signal may have been much less than the mean noise level itself. The measured power will be accurate to within $1.96\sigma/\sqrt{N}$ of the true power for 95% of the data. In the worst case, for which the signal only just exceed 7 times the standard error, the error in these 95% of cases will be less than +/−1.5 dB (i.e., 10.0 log [7/(7 − 1.96)]). The measured power will be accurate to within $3\sigma/\sqrt{N}$ for 99.75% of the data.

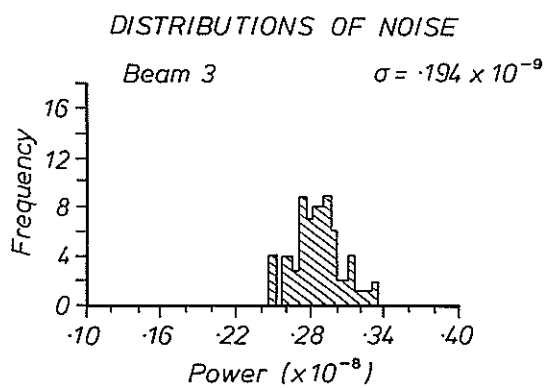

Fig. 3. Typical histogram of frequency of occurrence of various levels of noise.

Figure 4 shows typical height profiles of the 6 min means of the powers for beams 1 and 2 as a function of time for the October data. The existence of well-defined layering is clear, and the layers have lifetimes in excess of 2–3 hours in many cases. Figure 5 shows the mean powers averaged over the first 2 hours of data, and arranged in such a manner that the positions of the profiles indicate the regions of the sky from which each profile was obtained.

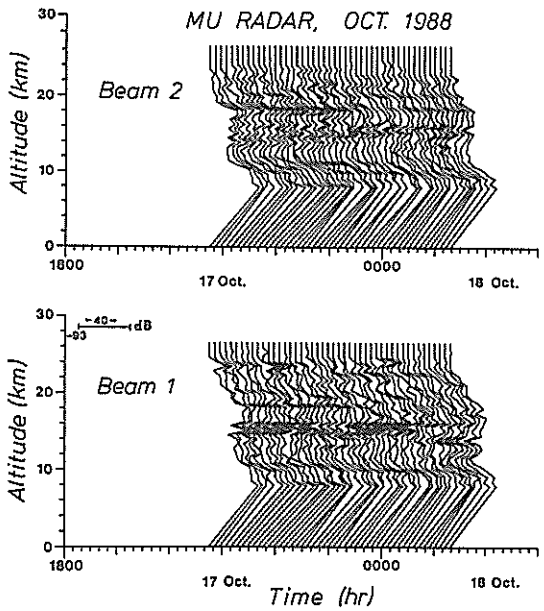

Fig. 4. Successive mean power profiles on beams 1 and 2. Each profile corresponds to an average over 8 × 45 s (or about 6 min). (Note that in this and all subsequent diagrams, the range has been converted to height.)

The profile on the vertical beam is also shown as a reference in each case. Note that the vertical coordinate is height, not range. Layering is clearly evident and the diagram shows well that horizontal layers extend over several km horizontally in the atmosphere.

Figure 6 shows mean profiles averaged over the whole observing periods for both the October and December data, and Figure 7 shows the ratio of power on each beam relative to that on the vertical beam at each height. The error treatment discussed above may be developed further to show that the errors in the aspect-ratios will be less than 1.5 dB at the greatest heights for each beam, and will fall to less than 0.5 dB within about 1.2 km of the top of the profile. It will be even smaller at lower heights. Most of the error will arise from the errors in power on the beam with the weakest signal; because the vertical beam power is always 5–10 dB greater than the power on the off-vertical beams, its relative error will be small. In the October case there is clear clustering into three distinct classes; the vertical beam, beams with tilts of 5°–7°, and beams with tilts in excess of 15°.

Assuming backscatter polar diagrams of the type exp $\{-\theta^2/\theta_s^2\}$, Figure 8 shows values of θ_s as a function of height. For the October data, two distinct classes appear; the beams closer to vertical show evidence for stronger aspect sensitivity than the beams tilted further off-vertical. The fact that θ_s is not the same on all beams may be interpreted as evidence that there are at least two types of scatterer, with the more aspect sensitive scatterers dominant overhead, and some more isotropic ones being important at larger angles. Indeed one might speculate that a continuum of scatterer shapes, ranging from moderately aspect-sensitive to almost isotropic, might exist. Such a model has been proposed independently by *Hocking et al.* [1984] (also see *Hocking* [1989]) and *Woodman and Chu* [1989], where they proposed that anisotropic scatterers exist near the top and bottom of turbulent layers and more isotropic ones dominate near the centre. There are also alternative models, and one of these will be discussed in more detail later. Although there are insufficient data in the October data to confirm it, one might suspect that the polar diagram of backscatter probably tends to flatten out at large values of tilt angle, as illustrated schematically on Figure 9*a*. To examine this issue in more detail, Figure 9*b* shows the variation of power as a function of beam tilt-angle and altitude for the December data. At many heights the power falls off relatively rapidly at tilt angles between 0° and 8° and then it does indeed flatten off at the larger angles. Similar trends have been noted by *Roettger et al.* [1981], *Doviak and Zrnic* [1984], and *Tsuda et al.* [1986]. Note that for the data shown on Figure 9*b*, the powers at the lowest six ranges and angles of 20° and 28° tilt are underestimates of the true power by about 2–3 dB, due to the effects of aliasing. (The filter function associated with coherent integration falls off quite quickly beyond the aliasing frequency, for example, *Schmidt et al.* [1979].)

Probably one of the more important results in this work is the evidence, seen in Figures 7 and 8, that the aspect sensitivity is strongest at 15- to 18-km altitude, and above that height there is a return to more isotropic scatter. At 15–18 km, θ_s becomes as small as 3°. Above and below, the minimum values of θ_s are more like 4°. Values for θ_s of 3°–4° imply scatterer half-lengths of 10–14 m, or scatterers with length to depth ratios of about 8–10 (since the optimum scale for h is 0.2 λ). This represents a fairly strong degree of anisotropy. Nevertheless, one might not consider such values as excessive, and anisotropic turbulence with such ratios could

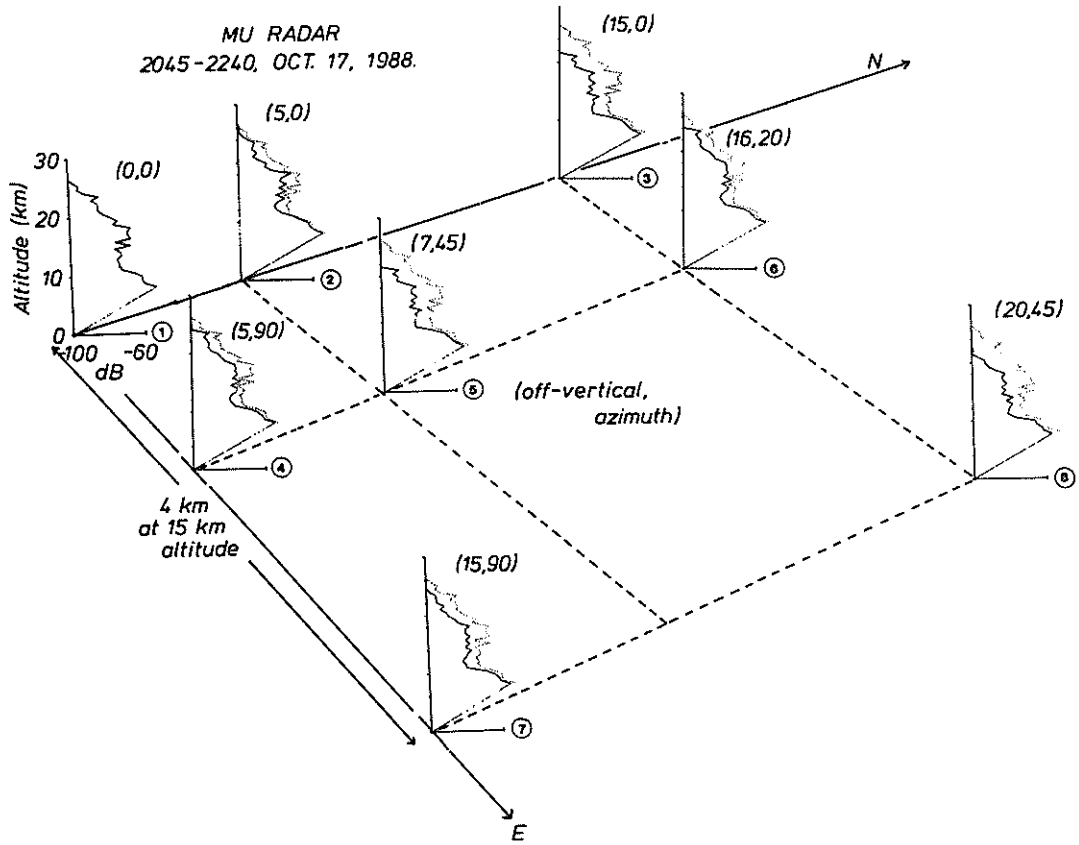

Fig. 5. Profiles of the mean power as a function of height, averaged over about the first 2 hours of data. The various profiles have been located in such a way as to indicate the relative horizontal displacements of the volumes of atmosphere from which they were sampled. In each case the profile for beam 1 (vertical beam) is shown as a reference (dotted line). The presence of layering is shown on all beams, and in many cases the peaks in power occur at the same heights on all beams. This illustrates that these layers have horizontal extents of at least several kilometers.

probably exist, as proposed, for example, by *Crane* [1980], *Doviak and Zrnic* [1984], and *Woodman and Chu* [1989]. For θ_s values of 2° and less the length to depth ratio is 16 and more. The mean value of θ_s at 15–18 km is around 3°, but some of the individual values contributing to this mean must have been even less. Thus although anisotropic turbulence can explain at least some of the observations presented so far, there is still room for doubt about it being the only cause; length-to-depth ratios of 20 or so might be hard to produce by turbulence alone. This issue will be addressed again in due course.

Another point worth noting is that the falloff in power as a function of angle between 0° and 8° is close to exponential (linear in decibels), rather than Gaussian (parabolic in decibels) and then tends to flatten off. This exponential decrease could be interpreted as the sum of the effects of many different scatterers with varying aspect ratios, but it might suggest that another model is more appropriate.

We must also be careful about our interpretation concerning the return to greater isotropy at greater heights. Because the signal-to-noise ratio was low at these heights, care must be taken to ensure that the effect is real. For example, if ground echoes are important, these might tend to be picked up equally on all beams (on average). Therefore sample time series of the (complex) amplitude were studied in detail. It was clear that over time intervals of 42 s the ground echoes did not fade but produced a constant offset. This is consistent with observations reported in earlier works [e.g., *Roettger et al.*,

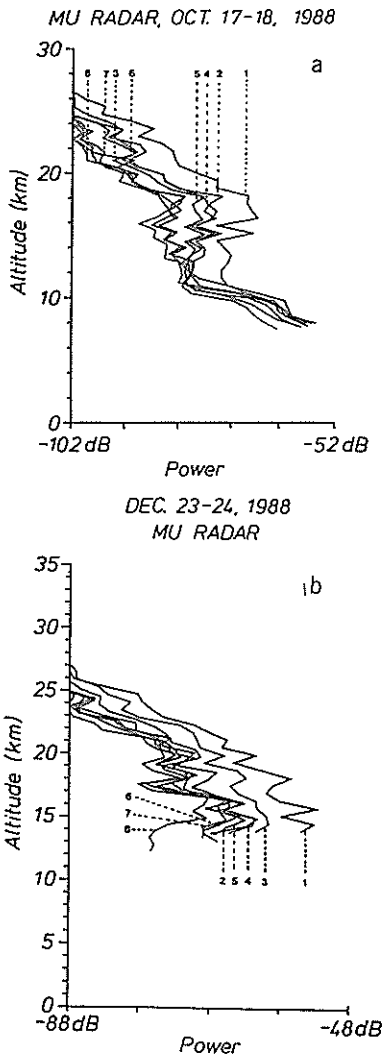

Fig. 6. Mean power as a function of height averaged over all available (aircraft free) data, for (*a*) October 17–18 (from 2045 October 17 to 0125 October 18) and (*b*) December 23–24 (from 2200, December 23 to 1030 December 24). Note the tendency for three distinct "clusters" of profiles in the October 17–18 case.

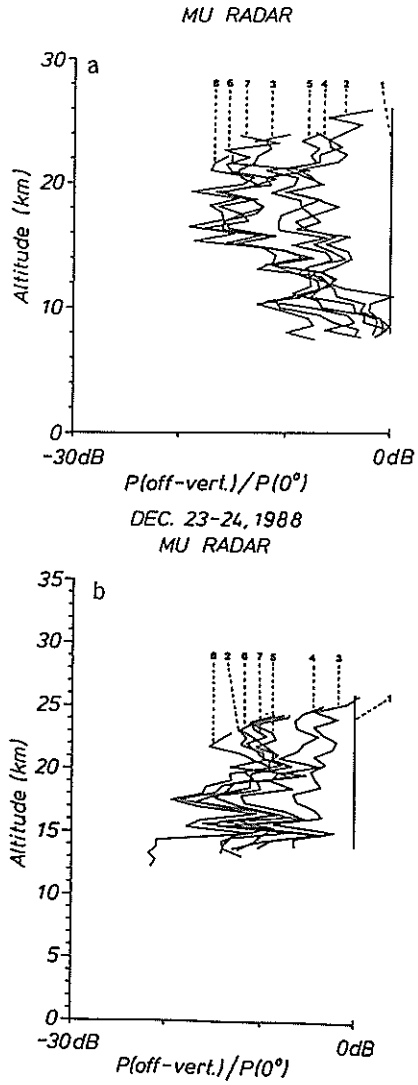

Fig. 7. Ratios of mean power on the indicated beams relative to the power on the vertical beam at the same heights for (*a*) October 17–18 and (*b*) December 23–24.

1981], although it is in contrast to the effect of ground echoes at UHF [e.g., *Sato and Woodman*, 1982*a*]. In calculating the mean scattered power this mean level was always removed first, so it is felt that ground echoes have been properly removed. It is also worth noting that the MU radar has very good side lobe suppression (better than 30 dB), which also helps to eliminate ground echoes.

Nevertheless, it is a worthwhile exercise to determine θ_s by other methods which do not depend on the absolute backscattered power. Two such methods and the subsequent results produced from using them are now described.

3.3. *Determination of θ_s by wind measurements*

As discussed in relation to (5), measurements of "horizontal" wind components by using tilted beams and assuming that the beam is tilted along the bore direction of the beam will be underestimates of the true horizontal velocity due to the effects of the aspect-sensitive scatter. Thus measurements of the "horizontal" velocity as a func-

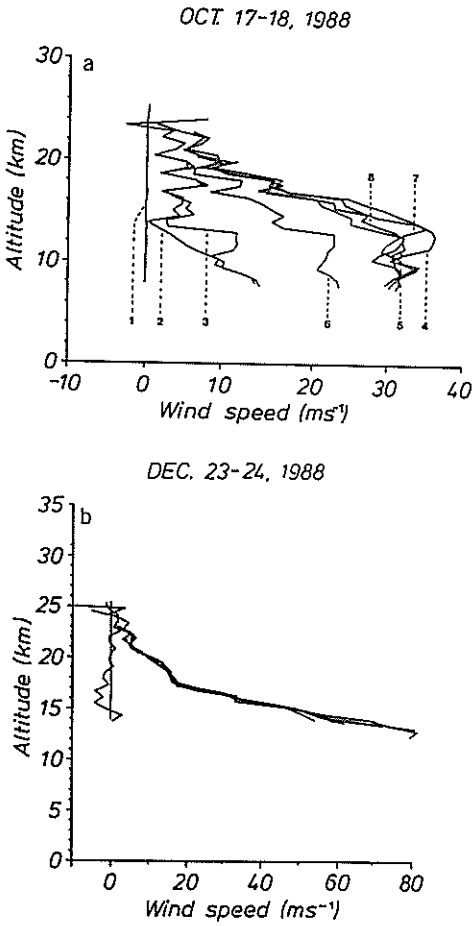

Fig. 10. Mean horizontal wind components in the azimuthal direction of the beam orientation for (*a*) October 17–18 and (*b*) December 23–24. In each case the wind has been calculated assuming isotropic scatter, so the effective pointing angle of the beam has been assumed to be the actual bore angle. For the vertical beam the actual radial (vertical) velocity is shown.

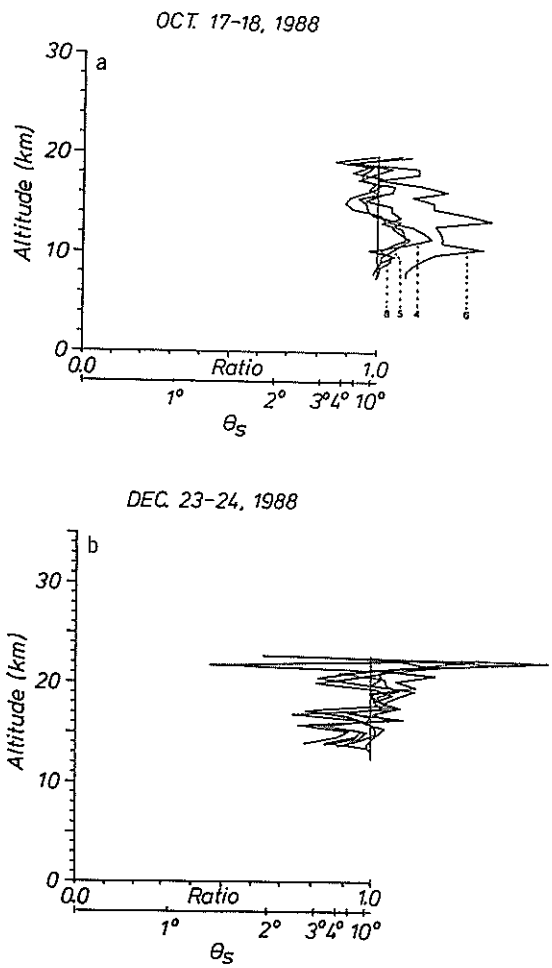

Fig. 11. θ_s values deduced from comparisons of the "horizontal" winds presented in Figure 10 for (*a*) October 17–18 and (*b*) December 23–24. Note that beam 2 for the October case has not been plotted, since it was different from the other northward beam at 10–14 km due to reasons which seemed to be geophysical.

in the December case. The northward beam show good agreement (beams 2 and 3 in the October case) at most heights, although there is a clear discrepancy at 10–14 km in the October data This is probably a geophysical effect, presumably due to a feature like a lee wave.

Figure 11 shows the ratio of the horizontal wind components relative to the "true" values where the true values were deduced using beams 3 (north) and 7 (east) for the October data and beams 2 (north) and 8 (east) for the December data. There is large scatter, and most of the values scatter about a ratio of 1.0. More importantly, in no case is there any strong indication of θ_s values as small as 2°. This is further confirmation that there is a range of scatterer aspect ratios, and the off-vertical beams with largest tilts "see" more isotropic scatterers. R_1 is also relatively insensitive to θ_T for θ_s values in excess of 3°–4° for the MU radar. Most of the observed fluctuations were therefore probably real geophysical fluctuations, and this is true even for beam tilts as small as 5°–7°. The fact that geophysical variations are more important than effects due to θ_s is encouraging for meteorological experiments which might be designed to look for spatial variations in wind strength with such a radar.

It is also noteworthy that these results are con-

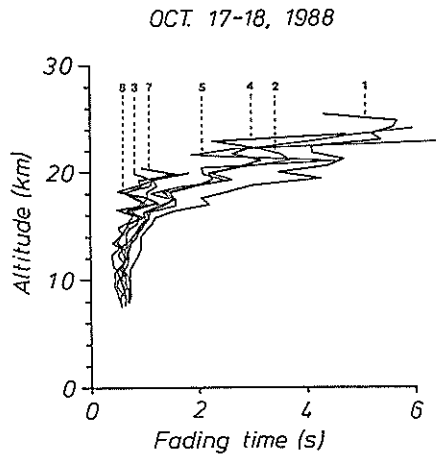

Fig. 12. Fading time $\tau_{0.5}$, as a function of height for October 17–18, averaged over the whole observing period.

sistent with *Tsuda et al.* [1986], where it can be seen that at tilt angles greater than 6°, the various estimates of the horizontal velocity agree to within about 3%. Conversion of the ratios in *Tsuda et al.* [1986, Figures 13 and 14] to values of θ_s gives values in excess of 6° for tilt angles greater than 5° from zenith.

3.4. *Determination of θ_s by fading times*

The third way in which estimates of θ_s can be made is to make use of the spectral widths. If the spectral broadening due to the horizontal motion of the scatterers through the beam is the main cause of the observed spectral width and exceeds the spectral broadening due to the fluctuating motions of the scatterers (as is often the case, especially in the stratosphere, for example, *Hocking* [1983*a*, 1986] and *Woodman and Chu* [1989]) then the observed spectral widths may be used to deduce R_2 in (7) and this, in turn, will allow estimates of θ_s to be made. For vertical beams this should work well if turbulence is weak and at least produce upper limits for θ_s. For off-vertical beams, other effects like fine-scale wind shears [e.g., *Sato and Woodman*, 1982*b*] and horizontal fluctuating motions [e.g., *Hocking*, 1983; *Hocking*, 1988, Appendix A] will produce extra broadening which may be important.

The spectral width has been determined as $0.22/\tau_{0.5}$, $\tau_{0.5}$ being the time lag for the autocorrelation function to fall to one half its zero-lag (noise removed) value. This formula has proved adequate in the past as a measure of the spectral half-power half-width [e.g., *Hocking*, 1986] and arises simply because the autocorrelation and power spectrum are Fourier transforms and are both often Gaussian in shape.

Plots of mean fading times as a function of height are shown in Figure 12 for the October data. Clearly, the fading time does depend on beam pointing angle, suggesting that fine-scale wind shears and horizontal motions are important as contributors to the spectral width. Values of R_2 can be deduced from these fading times provided the mean wind speeds are known. Figure 13 shows the resulting values for R_2 determined by adopting the horizontal wind values deduced using the beams with the largest tilts. Note that on all off-vertical beams the value of R_2 generally is around 1.0 or exceeds it. But for the vertical beam, the profile shows θ_s values as low as 1.5°–2°, with a minimum at 15- to 18-km altitude and an increase above. Thus the method is very sensitive to the scatter from around the vertical or in another words, the scatterers with the largest aspect-ratio. The fact that the values of θ_s are somewhat smaller than those deduced by the power-method highlights this and shows that there are indeed some scatterers which

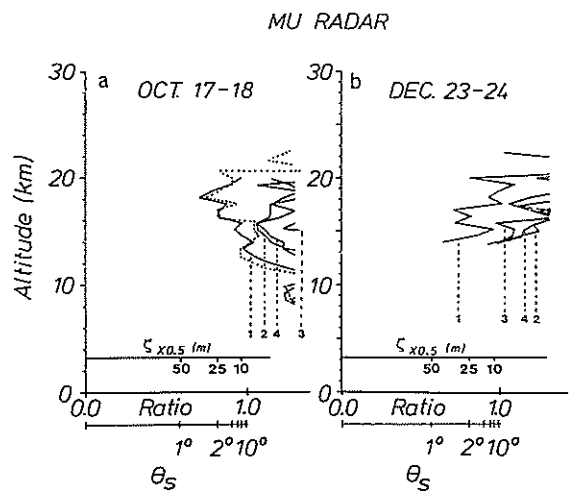

Fig. 13. θ_s values deduced by comparing the spectral width (determined from the fading times) to the spectral width expected due to the beam-broadening which would have been produced by isotropic scatterers. (*a*) Shows the October data and (*b*) the December data. Only a few beams are shown; while the measurements are very reliable when using the vertical beams the effects of fine-scale (unresolved) wind shears and horizontal fluctuating motions produce significant extra broadening for the off-vertical beams and render the determinations less useful.

are highly anisotropic with horizontal correlation lengths in excess of 35 m. If one adopts the picture that the scatter is due to elongated structures with ellipsoidal correlation functions of the type described by (2), then this means length-to-depth ratios will be in excess of 20. The picture of a continuum of scatterer shapes ranging from such anisotropic structures to almost isotropic scatterers is reinforced, and clearly, the different techniques which we have adopted are sensitive to different classes of scatterer. Of course, this model of turbulent scatterers is not the only which might describe the scatterers, but it is one which has been commonly used in the literature. Another will be discussed shortly.

In support of the above conclusions it is also worth recalling that *Tsuda et al.* [1986] examined individual spectra recorded with the MU radar, and for tilt angles of 2°–4° at 13-km altitude the spectra showed relatively sharp peaks near 0 Hz (*Tsuda et al.*, 1986, Figure 11). This is further support for the model of highly anisotropic scatterers embedded in more isotropic scatterers.

The return to greater isotropy at greater heights only occurs at one or two of the uppermost heights, and it is important to check whether this is real. Because the horizontal winds used to produce Figure 13 were measured with beams with the largest tilt, the signal-to-noise ratio fell to unacceptable values at lower heights than for beams near-vertical. Therefore R_2 has been recalculated using horizontal winds determined from beams with tilts nearer vertical. We have already seen that these winds are as reliable as those determined using the beams with larger tilts (Figures 10 and 11). The results of these additional calculations are shown in Figure 13 for the vertical beam for the October data as the broken line. The same trends are evident as for the solid line, but the data are extended by several height steps and the return to isotropy at the upper heights is clearer.

4. DISCUSSION

The results presented so far have shown that if the scatterers are modeled as perturbations of refractive index with Gaussian cross sections and with elliptical contours of constant refractive index (as described in (1)), then there is not one common length-to-depth ratio for the scatterers but rather a continuum of shapes. Beams tilted at different angles are sensitive to different scatterers. Such a model could explain some of the features described, and *Hocking et al.* [1984], *Hocking* (1985, p. 1418; *Hocking*, 1989] and *Woodman and Chu* [1989] have proposed that turbulent layers contain such a range of shapes, with the more anisotropic scatterers occurring near the top and bottom of the turbulent layers. Modeling work due to *Peltier et al.* [1978] and *Klaassen and Peltier* [1985] has also shown that such a picture may be realistic, since they noted very stable regions at the tops and bottoms of the layers which they generated in their models. It is probable that this situation applies at least in some instances.

Nevertheless, there are some points about the observations which might suggest that, at least on some occasions, such a model does not apply. Firstly, the fall off in power as a function of angle at small angles (less than say 8°) does not always seem to be Gaussian but is often exponential. Secondly, at some heights, and in particular at 15- to 18-km altitude, the horizontal correlation length based on averages performed using several hours of data can be in excess of 30 m. Presumably, it can be even more for short periods of time. This represents a length-to-depth ratio for the scatterers in excess of 20, and in such cases we must ask whether turbulence is capable of producing and maintaining such anisotropic structures. Indeed, data were examined at time scales of a few minutes, and the existence of scatterers with lifetimes of about 5 min and fading times in excess of 10–20 s at 15–18 km were found. This represents a value for θ_s of less than 1° and a correlation half-length of over 60 m. These results will be discussed in more detail in a later paper. However, the result certainly does suggest that we must also look at other models.

One model which may be important is the proposal that the scattering structures are not in fact always turbulent eddies but can be waves in the atmosphere. *Hines* [1960] and *Vanzandt and Vincent* [1983] have proposed that a spectrum of small-scale gravity waves may cause some of the scatter, and more recently *Klostermeyer* [1989] has noted that such small-scale buoyancy waves are produced when larger scale waves "break down" by nonlinear processes. It is not our intention to comment more about this model in this paper, but it will be discussed in a later paper. Suffice it to say that the model of turbulent scatter does not always apply, and we have already seen some evidence for this in

the form of very large aspect-ratios for the scatterers.

Regardless of the cause of the aspect-sensitivity of the scatterers the return to near-isotropy at greater heights above 18 km is no doubt important for the dynamics of the atmosphere. For example, it might be an indicator that buoyancy waves are beginning to "saturate" even at these low heights in the atmosphere, and if this is so it may mean that there is a transfer of momentum from the waves to the mean flow even at 20 km. A considerable amount of extra work is needed in order to determine just what this change in aspect-ratio means for the atmosphere but it cannot be ignored and will have at least some implications for the dynamics of the atmosphere. It is also worth noting that the turbulent diffusion coefficient in the atmosphere has a local minimum at 15–18 km [e.g., *Chakrabarty et al.*, 1987, Figure 5], and since the levels of turbulence are weakest there, it may allow a greater degree of stability and therefore allow more anisotropic scatterers to be stable.

5. CONCLUSIONS

It has been shown in this work that aspect sensitivity of VHF radio wave backscatter is strongest at 15- to 18-km altitude, where the effective backscatter polar diagram of the most anisotropic scatterers can have a $1/e$ half-width of less than 2°. This corresponds to horizontal correlation lengths of the refractive index fluctuations in excess of 25–30 m. (Note that this value refers only to the horizontal correlation length of the radar scatterers, i.e., those irregularities with vertical extents of the order of one half of a radar wavelength. The horizontal correlation lengths for scatterers of other vertical extents will be different.) Equally important, at any one height there is not one scatterer shape but rather a range of length-to-depth ratios exists, and the radar selects different scatterers preferentially depending on its tilt direction. Beams tilted at angles greater than about 10° detect almost isotropic scatter. At altitudes above 18 km the scatterers are more isotropic than below, with horizontal correlation lengths of typically less than 15 m. This return to isotropy suggests that buoyancy waves may be beginning to saturate significantly at heights of around 20 km, thereby generating turbulence and reducing stability. The above results have been obtained from studies of the backscattered power as a function of tilt angle, as well as studies of the radial velocities measured with the radar and the spectral widths relative to beam broadening. Although some of the data may be consistent with anisotropic turbulence, the large horizontal correlation lengths at 15–18 km suggest that there are also other types of scatterers, perhaps in the form of stratified steps or produced by buoyancy waves. The exponential fall off of power as a function of angle between 0° and about 10° is also noteworthy, but it is yet to be determined just what this means in terms of a physical model. In a later paper a stronger case will be made for the existence, at least on some occasions and at some heights, of "specular" reflectors which are not related to turbulence; in this work we merely note that while some of the scatter is probably due to anisotropic turbulence, it does not seem that all the scatter is due to such irregularities, and the occurrence of specular reflectors cannot be ruled out.

REFERENCES

Booker, H. G., J. A. Ratcliffe, and D. H. Shinn, Diffraction from an irregular screen with applications to ionospheric problems, *Phil. Trans. Roy. Soc.*, *A242*, 579–607, 1950.

Briggs, B. H., Diffraction by an irregular screen of limited extent, *Proc. Phys. Soc.*, *77*, 305–317, 1961.

Briggs, B. H., and R. A. Vincent, Some theoretical considerations on remote probing of weakly scattering irregularities, *Australian J. Phys.*, *26*, 805–814, 1973.

Chakrabarty, D. K., G. Beig, J. S. Sidhu, H. Chakrabarty, R. Narayanan, N. K. Modi, S. R. Das, and P. Chakrabarty, Measurements of the eddy diffusion coefficient in the middle atmosphere from a balloon at low altitude, *J. Atmos. Terr. Phys.*, *49*, 975–980, 1987.

Crane, R. K., A review of radar observations of turbulence in the lower stratosphere, *Radio Sci.*, *15*, 177–193, 1980.

Doviak, R. J., and D. S. Zrnic, Reflection and scatter formula for anisotropically turbulent air, *Radio Sci.*, *19*, 325–336, 1984.

Fukao, S., T. Sato, T. Tsuda, S. Kato, K. Wakasugi, and T. Makihira, The MU radar with an active phased array system, 1, Antenna and power amplifiers, *Radio Sci.*, *20*, 1155–1168, 1985*a*.

Fukao, S., T. Tsuda, T. Sato, S. Kato, K. Wakasugi, and T. Makihira, The MU radar with an active phased array system, 2, Inhouse equipment, *Radio Sci.*, *20*, 1169–1176, 1985*b*.

Gage, K. S., and J. L. Green, Evidence for specular reflection from monostatic VHF radar observations of the stratosphere, *Radio Sci.*, *13*, 991–1001, 1978.

Gage, K. S., B. B. Balsley, and J. L. Green, Fresnel scattering model for the specular echoes observed by VHF radars, *Radio Sci.*, *16*, 1447–1453, 1981.

Green, J. L., and K. S. Gage, Observations of stable layers in the troposphere and stratosphere using VHF radars, *Radio Sci.*, *15*, 395–405, 1980.

Hines, C. O., Internal atmospheric gravity waves of ionospheric heights, *Can. J. Phys.*, *38*, 1441–1481, 1960.

Hocking, W. K., On the extraction of atmospheric turbulence parameters from radar backscatter Doppler spectra, 1, Theory, *J. Atmos. Terr. Phys.*, *45*, 89–102, 1983.

Hocking, W. K., Measurement of turbulent energy dissipation rates in the middle atmosphere by radar techniques: A review, *Radio Sci.*, *20*, 1403–1422, 1985.

Hocking, W. K., Observation and measurement of turbulence in the middle atmosphere with a VHF radar, *J. Atmos. Terr. Phys.*, *48*, 655–670, 1986.

Hocking, W. K., Radar studies of small scale structure in the upper middle atmosphere and lower ionosphere, *Adv. Space Res.*, *7*, 327–338, 1987.

Hocking, W. K., Two years of continuous measurements of turbulence parameters in the upper mesosphere and lower thermosphere made with a 2-MHz radar, *J. Geophys. Res.*, *93*, 2475–2491, 1988.

Hocking, W. K., Target parameter estimation, *Middle Atmos. Program Handb.*, in press, 1989. (Also presented at the International School of Atmospheric Radar, Kyoto, Nov. 24–28, 1988).

Hocking, W. K., and Roettger, J., Pulse-length dependence of radar signal strengths for Fresnel backscatter, *Radio Sci.*, *18*, 1312–1324, 1983.

Hocking, W. K., R. Ruester, and P. Czechowsky, Observation and measurement of turbulence and stability in the middle atmosphere with a VHF radar, *Rep. ADP 335*, Univ. of Adelaide, Dep. of Phys., Adelaide, South Aust., 1984.

Hocking, W. K., R. Ruester, and P. Czechowsky, Absolute reflectivities and aspect sensitivities of VHF radio wave scatterers measured with the SOUSY radar, *J. Atmos. Terr. Phys.*, *48*, 131–144, 1986.

Hocking, W. K., P. T. May, and J. Roettger, Interpretation, reliability and accuracies of parameters deduced by the spaced antenna method in middle atmosphere applications, *Pure Appl. Geophys.*, *130*, 571–604, 1989.

Klaassen, G. P., and W. R. Peltier, Evolution of finite amplitude Kelvin-Helmholtz billows in two spatial dimensions, *J. Atmos. Sci.*, *42*, 1321–1339, 1985.

Klostermeyer, J., On the role of parametric instability the MST radar observations of mesospheric gravity waves, *Middle Atmos. Program Handb.*, *28*, 299–308, 1989.

Peltier, W. R., J. Halle, and T. L. Clark, The evolution of finite-amplitude Kelvin-Helmholtz billows, *Geophys. Astrophys. Fluid Dyn.*, *10*, 53–87, 1978.

Ratcliffe, J. A., Some aspects of diffraction theory and their application in the ionosphere, *Rep. Prog. Phys.*, *19*, 188–267, 1956.

Roettger, J., Reflection and scattering of VHF radar signals from atmospheric refractivity structures, *Radio Sci.*, *15*, 259–276, 1980.

Roettger, J., and C. H. Liu, Partial reflection and scattering of VHF radar signals from the clear atmosphere, *Geophys. Res. Lett.*, *5*, 357–360, 1978.

Roettger, J., P. Czechowsky, and G. Schmidt, First low-power VHF radar observations of tropospheric, stratospheric and mesospheric winds and turbulence at the Arecibo Observatory, *J. Atmos. Terr. Phys.*, *43*, 789–800, 1981.

Sato, T., and R. F. Woodman, Spectral parameter estimation of CAT radar echoes in the presence of fading clutter, *Radio Sci.*, *17*, 817–826, 1982*a*.

Sato, T., and R. F. Woodman, Fine altitude resolution observations of stratospheric turbulent layers by the Arecibo 430 MHz radar, *J. Atmos. Sci.*, *39*, 2553–2564, 1982*b*.

Schmidt, G., R. Ruester, and P. Czechowsky, Complementary code and digital filtering for detection of weak VHF radar signals from the middle atmosphere, *IEEE Trans. Geosci. Electr.*, *GE-17*, 154–161, 1979.

Tsuda, T., T. Sato, K. Hirose, S. Fukao, and S. Kato, MU radar observations of the aspect sensitivity of backscattered VHF echo power in the troposphere and lower stratosphere, *Radio Sci.*, *21*, 971–980, 1986.

VanZandt, T. E., and R. A. Vincent, Is VHF Fresnel reflectivity due to low frequency buoyancy waves?, *Handbook for MAP*, vol. 9, pp. 78–80, SCOSTEP Secr., Univ. of Ill., Urbana, 1983.

Woodman, R. F., and Y.-H. Chu, Aspect sensitivity measurements of VHF backscatter made with the Chung-Li radar: Plausible mechanisms, *Radio Sci.*, *24*, 113–126, 1989.

S. Fukao, S. Kato, T. Sato, T. Tsuda, and M. Yamamoto, Radio Atmospheric Science Center, Kyoto University, UJI, Kyoto 611, Japan.

W. K. Hocking, Department of Physics and Mathematical Physics, University of Adelaide, GPO Box 498, Adelaide, South Australia 5001.